NMR SPECTROSCOPY OF GROUP 13 METAL IONS: BIOLOGICALLY RELEVANT ASPECTS

J. P. André [a *], H. R. Mäcke [b]

[a] Centro de Química, Universidade do Minho, Campus de Gualtar, 4710 Braga, Portugal

[b] Division of Radiological Chemistry, Nuclear Medicine, University Hospital of Basel, 4 Petersgraben, 4031 Basel, Switzerland

Keywords: ^{27}Al NMR, biological systems, Group 13 elements, MRI, macrocyclic complexes

* Corresponding author: Tel.: +351-253-604-385, fax: +351-253-678-983.
E-mail address: jandre@quimica.uminho.pt

Abstract

In spite of the fact that Group 13 metal ions (Al^{3+}, Ga^{3+}, In^{3+} and $Tl^{+/3+}$) show no main biological role, they are NMR-active nuclides which can be used in magnetic resonance spectroscopy of biologically relevant systems. The fact that these metal ions are quadrupolar (with the exception of thallium) means that they are particularly sensitive to ligand type and coordination geometry. The line width of the NMR signals of their complexes shows a strong dependence on the symmetry of coordination, which constitutes an effective tool in the elucidation of structures.

Here we report published NMR studies of this family of elements, applied to systems of biological importance. Special highlighting is given to the binding studies of these cations to biological molecules, like proteins, and to chelating agents of radiopharmaceutical interest. The possibility of *in vivo* NMR studies is also stressed, with extension to ^{27}Al-based MRI (magnetic resonance imaging) experiments.

1. Introduction

In the last decades the magnetic resonance techniques have evolved as essential tools for research and practice in domains like chemistry, biochemistry, biology, pharmacy and medicine [1-5]. In this review we report both *in vitro* and *in vivo* NMR and magnetic resonance imaging (MRI) studies based on the Group 13 metals, mainly published during the last decade.

Although none of the Group 13 elements is considered as essential to life, their trivalent ions are, nonetheless, of high biological interest. The redox chemistry of thallium is considerably different from the other elements of the group; under standard conditions the most stable oxidation state is Tl^{+}, although the divalent and the trivalent states may exist under biological conditions.

Aluminum is the most abundant metal on earth and the natural element consists entirely of the ^{27}Al isotope. It is a nonessential element that only in the last three decades started being considered a potential toxic element with a possible link to neurological problems like Alzheimer's disease and dialysis encephalopathy, and also to some bone disorders and problems in the haematopoietic system, muscles and joints [6,7]. Overall it seems that the intake of aluminum by humans (food, water,…) is between 2 and 20 mg of the element per day. The normal human aluminum burden in an adult is about 20-50 mg but it can be 2 g in patients with encephalopathy syndrome. Normal blood plasma aluminum concentration is about 0.005 mg/L. Blood contains less than 1% of the aluminium body burden, of which about 80% is bound to proteins. It accumulates in tissues mainly in liver, bones and spleen of humans and animals.

Due to the increasing acidity of the environment and concomitant dissolution of aluminum minerals, the concentration of this element in fresh waters can rise considerably. As Williams points out [8], the continuous study of the aluminum's chemistry and of its interaction with biological molecules *in vitro* and *in vivo* is a necessary precaution.

The review of Orvig [9] on the coordination chemical aspects of aluminum, compiles literature data available until the very early nineties. Among other aspects this review includes ^{27}Al NMR studies on the interaction of Al^{3+} with biologically relevant carboxylate type ligands. These ligands are of particular importance in view of their occurrence in natural waters and to the fact that citric acid is the main low-molecular-weight carrier of aluminum in blood.

Gallium and indium have a very similar chemistry and neither has a natural metabolic role. Gallium is present in human tissues at a level of only 10^{-4} to 10^{-3} ppm [10]. It has two naturally occurring isotopes (^{69}Ga, 60.5%; ^{71}Ga, 39.5%) and thirteen radioactive nuclides. ^{67}Ga and ^{68}Ga are two radioisotopes with the appropriate energies and half-lives for

γ-scintigraphy and positron emission tomography (PET), respectively. ^{111}In is also a radionuclide which is widely employed in nuclear medicine for γ-imaging. These radioisotopes are administered to the patients in the form of stable chelates.

Thallium salts are poisonous due to the ability of the thallous ion to mimic alkali metal ions, especially K^+. In addition Tl^+ ion is absorbed efficiently from the human gastrointestinal tract [11].

2. NMR properties

^{27}Al, $^{69/71}$Ga and $^{113/115}$In are magnetically active isotopes. They are characterised by a high sensitivity to detection by NMR and large chemical shift ranges, two factors that make their study relatively easy. They are quadrupolar nuclei (spin I >1), which rather than being undesirable can give much structural information. The relaxation of a quadrupolar nucleus is mainly due to the interaction of the quadrupole moment with electrical field gradients present at the position of the nucleus. This interaction allows an efficient transfer of energy from the nucleus to the molecular rotational motions. In the limit of fast motion, the nuclear spin quadrupolar relaxation follows the equation:

$$\frac{1}{T_{1Q}} = \frac{1}{T_{2Q}} = \frac{3\pi^2}{10} \cdot \frac{2I+3}{I^2(2I-1)} \cdot \left(1+\frac{\eta^2}{3}\right) \cdot \left(\frac{e^2 qQ}{h}\right)^2 \cdot \tau_C$$

where T_{1Q} and T_{2Q} are the quadrupolar spin-lattice and spin-spin relaxation times respectively; I is the nuclear spin; e^2qQ/h is the quadrupolar coupling constant; q is the electric field gradient at the nucleus; e is the charge of the electron; Q is the nuclear electric quadrupole moment; h is the Planck's constant; τ_C is the rotational correlation time. η is an asymmetry parameter ($0<\eta<1$) that gives the deviation of the electric field gradient from axial symmetry, which mainly depends on the lack of spherical symmetry of the p electrons density. The electric field gradient is a very important parameter in the relaxation of quadrupolar nuclides.

Cubic, tetrahedral, octahedral or spherical symmetry have in principle a zero field gradient (q = 0), which gives origin to sharp signals. Asymmetry in the ligand field produces an increase in the NMR line width [12,13].

^{27}Al has shown to be more amenable to NMR studies than its companion elements due to a higher receptivity and the existence of only one isotope as shown in Table 1. Another attractive feature of this nucleus is the relatively small quadrupolar moment associated with a high nuclear spin (I=5/2). These two favourable factors result in a much higher relative peak height – by one order of magnitude or more than the other elements of the group. This means that sufficient signal/noise ratios can be obtained even with dilute (≈ 0.01 M) solutions of aluminum compounds. ^{27}Al line widths may vary from 3 Hz to several kilohertz, and the signal may even completely vanish into the base line noise in some instances. This negative aspect of quadrupolar relaxation is counterbalanced by the additional information obtained about molecular symmetries from the magnitude of quadrupolar line broadenings. The range of ^{27}Al NMR chemical shifts is ~ 450 ppm.

Gallium has two naturally occurring isotopes, ^{69}Ga and ^{71}Ga, with nuclear spin I=3/2. ^{71}Ga has higher receptivity and narrower line width than the former one (Table 1), which means that ^{71}Ga is usually the more favourable isotope for direct NMR observations in spite of the low natural abundance. The chemical shift range of the gallium nucleus is approximately 1400 ppm [14].

^{113}In and ^{115}In have large quadrupole moments which make their line widths very sensitive to the environmental symmetry of the indium nucleus. The low receptivity of ^{113}In accounts for almost no NMR studies based on this nuclide. The chemical shift range of the indium nucleus is approximately 1100 ppm [15].

^{203}Tl and ^{205}Tl are the only non-quadrupolar NMR active nuclei in the Group 13 family, and have high receptivities - ^{203}Tl being slightly less receptive than ^{31}P, while ^{205}Tl, the third most

receptive spin I=1/2 nuclide, is twice as receptive as ^{31}P. Because of its similarities to the alkaline metal ions, the Tl^+ ion has potential as probe for studies of Na^+ and K^+ functions in biological systems.

3. Binding of the metal ions to biological molecules

3.1 Proteins

NMR spectroscopy has shown to be a convenient way to study proteins in solution and, among them, transferrins have deserved a special attention by researchers [16]. These proteins are too big for complete structural determination in solution by current multidimensional NMR techniques (^1H NMR signals are intrinsically broad due to slow molecular tumbling) but ^{27}Al, $^{71/69}Ga$ and ^{205}Tl NMR can be used to investigate directly the metals in their specific binding sites and to reveal subtle intersite differences. Human serum transferrin is the protein that transports Fe^{3+} ions and it is a member of a small group of monomeric non-heme proteins (MW *circa* 76-81 k), which includes lactoferrin, ovotransferrin and melanotransferrin. It has two binding sites for ferric ions (these are found in a six-coordinate, distorted octahedral coordination geometry) which are identified as C-terminal and N-terminal sites. Two tyrosines, one histidine, and one aspartic acid constitute four ligating groups to the metal ion. It requires a synergistic anion for the formation of stable metal complexes (*in vivo* the CO_3^{2-} as a bidentate ion serves this purpose by coordinating directly to the metal in the fifth and sixth coordination positions). Since serum transferrin is normally only about 30% saturated with iron, it retains a relatively high capacity for binding other metal ions. Due to its high NMR receptivity, the $^{205}Tl^{3+}$ NMR signals of protein-bound Tl^{3+} ions can be observed even at mM concentrations. The first ^{205}Tl NMR study of human serum transferrin (sTf) was reported twenty years ago by Bertini *et al* [17]. These authors showed that ^{205}Tl NMR is a convenient probe to monitor the occupancy of the two available binding sites of transferrin and

characterised the dithallium(III)-transferrin and the monothallium derivatives with bicarbonate as synergistic ion. The high affinity of the protein for trivalent metal ions was thought to be responsible for the stabilization of the 3+ oxidation state of the metal. Two distinct ^{205}Tl NMR signals (+2075 and +2055 ppm), of similar shape, were found for the $(Tl^{3+})_2$Tf derivative at physiological pH. The two signals are relatively broad and show a different pH dependence (the signal with the smaller chemical shift showed to be more resistant to acidification). At physiological pH the Tl^{3+} ion was shown to bind sequentially to the two sites; the signal with smaller chemical shift appears first and it was assigned to Tl^{3+} bound to the acid-resistant C-terminal site. The signal showing a larger chemical shift was assigned to the Tl^{3+} bound to the N-terminal site. Using ^{13}C NMR spectroscopy for the study of the ^{205}Tl-Tf-$^{13}CO_3$ derivative the same group showed that the ^{13}C nucleus of the synergistic anion is strongly magnetically coupled to the ^{205}Tl nucleus so that its ^{13}C signal is split into a doublet. This result constituted an evidence of carbonate coordination to the metal [18].

Aramini and Vogel [19] also examined the binding of Tl^{3+} to human sTf and additionally investigated its binding to chicken ovotransferrin (oTf) in the presence of carbonate and oxalate by ^{205}Tl and ^{13}C NMR. They found two ^{205}Tl NMR signals for $(Tl^{3+})_2$-Tf when the synergistic anion is carbonate, due to the bound metal ion in the two high-affinity iron binding sites of each protein (at +2055 and +2072 ppm for sTf and +2075 and +2045 ppm for oTf). When the same adducts were prepared with ^{13}C-enriched carbonate it was possible to find two closely spaced doublets in the carbonyl region of the ^{13}C NMR spectrum of sTf which correspond to the labelled anion directly bound to the metal ion in both sites of the protein. In the ^{13}C NMR spectrum of the analogous compound of oTf only one doublet was found. The magnitudes of the spin-spin coupling between the bound metal ion and carbonate - $^2J(^{205}Tl\text{-}^{13}C)$ - were in the range of 270-290 Hz. Use of the proteolytic half-molecules of oTf and the recombinant N-terminal half molecule of sTf allowed to assign the ^{205}Tl and ^{13}C NMR

signals due to the bound metal ion and anion in both proteins. Titration studies made possible to conclude that Tl^{3+} is bound with a higher affinity to the C-terminal site of sTf, whereas no site preference could be noted for oTf. If oxalate was used as synergistic anion, the ^{205}Tl NMR signals arising from the bound metal ion in the sites of oTf were shifted downfield and became almost degenerate (+2103 and +2100 ppm). A very complex pattern of signals was found for $^{13}C_2O_4^{2-}$ in the ^{13}C NMR spectra of both proteins which was related to the bidentate binding of oxalate to the metal ion.

In another study Vogel and Aramini [20] demonstrated the feasibility of using ^{27}Al NMR to probe Al^{3+} binding to transferrins using the quadrupolar central transition NMR approach (1/2→-1/2 transition). The chemical shifts of the ^{27}Al signals due to oTf-bound Al^{3+} were found to be within the range +40 to -46 ppm, which is in accordance with a six-coordinate (octahedral) Al^{3+} complex. They pointed out that the detectability of the central transition of quadrupolar nuclei bound to large proteins depends considerably on a number of factors: (i) the strength of the external magnetic field (ω_0); (ii) the dimensions and motion of the macromolecule (τ_c, temperature, solution viscosity), (iii) the intrinsic quadrupole moment of the specific nucleus (Q), and (iv) the nature of the electric field gradient at the metal ion binding site. Other studies performed by the same authors, based on transferrin-bound metals, have illustrated some features the ^{27}Al and $^{71/69}Ga$ NMR signals of these compounds [21-23]. Gallium NMR studies with oTf have shown that the metal ion interacts preferentially with the N-site of protein, as previously found for the Al^{3+} binding to oTf and human sTf, when carbonate serves as the synergistic anion. Moreover, the isotropic chemical shifts of the oTf-bound $^{71/69}Ga$ NMR signals fall well within the range of Ga^{3+} bound to six oxygen-containing ligands (+40 to +80 ppm).

The interaction of monovalent thallium with yeast pyruvate kinase (yPK) was investigated by $^{205}Tl^{+}$ NMR [24]. Pyruvate kinase from almost all sources requires both monovalent and

divalent metal ions. Potassium is the physiologically important cation but numerous monovalent cations, including Tl^+, can also activate this enzyme. In this work it was shown that $TlNO_3$ activates yPK to 80-90% activity compared to KCl in the presence of $Mn(NO_3)_2$ as the activating divalent cation. At higher concentrations of Tl^+, enzyme inhibition is observed and the extent of this inhibition was found to be dependent on the nature and concentration of the divalent cation. The effect of Mn^{2+} on the $1/T_1$ and $1/T_2$ values of $^{205}Tl^+$ in the presence of yPK was determined at different frequencies. The temperature dependence of the relaxation rates indicated that fast exchange conditions prevail for $^{205}Tl^+$ longitudinal relaxation rates. The correlation time, τ_c, for the Mn^{2+}-$^{205}Tl^+$ interaction was estimated by a frequency dependence of $1/T_{1m}$ for several enzyme complexes, and an average value of 0.91 ns was found. The distance between Tl^+ and Mn^{2+} at the active site of yPK was calculated from the paramagnetic contribution of Mn^{2+} to the longitudinal relaxation rates of Tl^+ bound to yPK. For the apo yPK complex, the Tl^+ to Mn^{2+} distance was found to be 6.7±0.2 Å.

3.2 Adenosine triphosphate

The interaction of Al^{3+} with biologically relevant phosphates is important [6]. In membrane systems, the Al^{3+} ion binds strongly to the phosphate head groups of the membrane. The neurotoxicity of Al^{3+} is also manifested by inhibiting certain enzymes, like ATPase. It is possible that the Al^{3+} ion, once bound to ATP, interferes with Mg^{2+}, so that any consequent reactions requiring the Mg^{2+}-ATP complex participation are inhibited. This has prompted the study of the binding of Al^{3+} to adenosine triphosphate (ATP) by ^{27}Al NMR. The line widths of these complexes typically fall within the range ~150-500 Hz. Dettelier and co-workers [25] studied these interactions at pH 7.4 using multinuclear NMR spectroscopy. The ^{27}Al NMR study allowed them to find two complexes coexisting in equilibrium: a 2:1 and a 1:1 complexes, $Al(ATP)_2$ and Al(ATP).

4. Complexes of the metal ions

4.1 Radiopharmaceuticals

^{67}Ga (γ, $t_{1/2}$ 3.25 days), ^{68}Ga (β^+, $t_{1/2}$ 68 min) and ^{111}In (γ, $t_{1/2}$ 2.82 days) are radionuclides that find a wide scope of applications in diagnostic radiopharmaceuticals due to their emitting properties and to their suitable half lives. They have to be chelated with suitable ligands that form kinetically and thermodynamically stable complexes *in vivo* or, otherwise, the radiometal, which is toxic, can be donated to endogenous high-affinity binding sites such as those located on the serum transferrin.

The triazamacrocyclic ligands with different types of pendant arms (carboxylates [26-29]; alkylphosphinates [30]; methylenephosphonates [31]) proved to be suitable ligands regarding the stable complexes they form with the Group 13 metal ions. The complexes formed are usually octahedral or pseudo-octahedral, showing a C_3 symmetry axis, with the three nitrogen atoms occupying one facial plane and the oxygen atoms from the pendant arms occupying the other (N_3O_3 systems). For this reason the complexes are highly symmetrical at the coordination centre and the metal ion gives origin to sharp resonance lines.

Parker and co-workers studied metal complexes of triazacycloalkane triacetic ligands with potential application in imaging and radioimmunotherapy [26-27]. A ^{71}Ga NMR spectroscopy investigation, both *in vitro* and *in vivo* in the liver of mice, proved that the complex Ga(NOTA) (see Chart 1 for ligand structures and the list of abbreviations for ligand names) has a remarkable stability with respect to acid-catalysed dissociation. The complex in the solid state is approximately octahedral and ^{1}H NMR studies suggested that this structure is maintained in solution. The pair of C_3–symmetric "facial" N_3 and O_3 donors lead to a minimal electric field gradient at the metallic centre in the "*x*-*y*" plane and consequently to the observation of the narrow ^{71}Ga resonance (+171 ppm, Table 2).

André *et al* demonstrated that the complex Ga(NODASA) complex, similarly to Ga(NOTA), shows a ^{69}Ga NMR signal typical of a pseudo-octahedral species (+165 ppm, Table 2) [28]. *In vitro* and *in vivo* ^{27}Al NMR spectroscopy with rats was used to study the complexes Al(NODASA) and Al(NOTA) [29] . Both chelates showed very high stability towards acid catalyzed dissociation and their ^{27}Al NMR resonances showed to be characteristic of highly symmetrical species with chemical shifts within the range for octahedral or pseudo-octahedral geometries (+47 and +49 ppm respectively). The thermodynamic stability of Al(NODASA) was estimated using ^{27}Al NMR spectroscopy ($\log K_{ML}$=18.50). The *in vivo* ^{27}Al NMR signals of both complexes was detected in the region of the liver of rats and the fact that the aluminum resonances of the complexes was still detectable in the urine indicated that they remain intact under physiological conditions and that they are mainly eliminated from the body through the kidneys [29].

Parker *et al* also investigated the coordination chemistry of indium and gallium with α-aminoalkylphosphinic acid ligands based on triazacyclononane ([9]aneN$_3$) skeleton (L1, L5 and L7 in Chart 1) and compared them with the analogous α-aminocarboxylate ligands [30]. The ^{71}Ga NMR signals of the phosphinate complexes appear at lower frequencies (between +130 and +140 ppm, Table 2) than the signal of Ga^{3+} in a tris(amino)tris(carboxylate) environment. Moreover, they found that increasing the size of the alkyl group on the phosphorus atom increased the ^{71}Ga line width (L7 in Table 2). As in each of these cases, the electric field gradient about the quadrupolar nuclei is very similar, the line width change was attributed to a change in molecular tumbling (τ_c).

Geraldes and co-workers performed a ^{71}Ga NMR study with a [9]aneN$_3$ derivative, exhibiting phosphonate arms (NOTP). This study showed the formation of a very symmetrical 1:1 $Ga(NOTP)^{3-}$ complex with a chemical shift of +110 ppm (Table 2) [31].

The structures of the Al^{3+}, Ga^{3+} and In^{3+} complexes of the polyamino polycarboxylate ligand TTHA and of its N,N'''-bis(butylamide) derivative were investigated by multinuclear ^{27}Al, ^{71}Ga and ^{115}In NMR spectroscopy [32]. It was found that the line widths of the metal resonances increased sharply in the above order, in agreement with the relative width factors for quadrupolar relaxation of those nuclei, which are 1.0:2.34:14.0. The results are summarised in Table 2.

When the oxygen donors are from phenolates, in tripodal aminophenolate ligand complexes (TAMS, TACS and TAPS in Chart 1), it was found that the chemical shift range of ^{71}Ga moves to even lower frequencies (+18 to +57 ppm) but still lie in the range that is expected for octahedral Ga^{3+} complexes [33]. The analogous aluminum complexes show the same trend. ^{115}In NMR signals were also observed in spite of the large line widths (Table 2).

Orvig *et al* [34] demonstrated the formation of highly symmetrical bicapped bisligand complexes of Group 13 metal ions with the N_4O_3 tripodal phosphonic ligand H_3ppma (Chart 1), which give very narrow signals in the ^{27}Al, ^{71}Ga and ^{115}In NMR spectra (Table 2) as a result of a S_6 symmetry. The complex $[AlL_2](NO_3)_3.2H_2O$ showed a rare example of a $^2J_{AlP}$ coupling pattern, which was observed in both ^{27}Al and ^{31}P NMR spectra.

4.2 Other complexes

^{27}Al NMR spectroscopy has also been successfully employed to study aluminum-containing complexes existing in natural waters. Casey *et al* studied the rates of solvent exchange in aqueous Al^{3+}-maltolate complexes. Maltolate is a natural product that can be isolated from larch trees but is now widely used as food additive. It is soluble in water, and tris-complexes of Al^{3+} with this ligand are toxic and cause brain disease. With the help of a multitemperature ^{27}Al NMR study it was shown that the maltolate labilizes the inner sphere water molecules of Al^{3+}-complexes by factors that are very similar to other bidentate ligands, such as methylmalonate, without reducing the overall charge of the Al^{3+}-complex [35].

5. ^{27}Al-based magnetic resonance imaging

The gastric emptying (GE) rate is a subject of great relevance in gastrointestinal medicine and pharmacology. The routine procedure to study the GE in clinical practice is to mark ion exchange resins with radioactive isotopes like ^{111}In or ^{99m}Tc. These isotopes are detected by γ–scintigraphic techniques. The standard magnetic resonance imaging (MRI) technique, which is based on the ^{1}H magnetic resonance of the water protons in the body, can be used as well in the study of GE. Seelig *et al* suggested an alternative imaging modality for the study of GE based on the ^{27}Al NMR signal [36]. These authors have shown that the $[Al(H_2O)_6]^{3+}$ is detectable by ^{27}Al NMR in the human stomach if aluminum containing drugs are ingested and the pH of gastric juice is lower than 4. Under these conditions the ^{27}Al resonance has a line width of only a few Hz. Aluminum containing drugs find widespread medical applications as astringents, antacids and antiulcer agents. *In vitro* ^{27}Al NMR studies of aluminum containing antacid preparations in HCl demonstrated that the Al^{3+} ion is released from these drugs [37]. Seelig *et al* demonstrated that the oral uptake of aluminum containing drugs in pharmaceutical doses and the time course of GE could be visualised *in vivo* using ^{27}Al MRI. Since a pH of 1-2 is typical for the gastric milieu and the remainder of the gastric emptying has a pH value of 6.0-7.4, the gastric lumen is ideally suited for the detection of ^{27}Al NMR signal devoid of background signals. They applied ^{27}Al MRI to visualize gastric pH and found that as little as 0.5 mg Al^{3+} could be detected in the human stomach [36]. More recently the same group reported the visualization of the stomach of humans and mice and the gastric emptying rate using aluminum-loaded ionic exchange resins [38]. For stomach emptying in mice the exponential decay constant was 74 min, whereas the half-time of the linear gastric emptying in humans was 30 min. The difference was explained with basis on the feeding patterns of human and mice. It was also found that the resin-bound Al^{3+} ion has magnetic properties

similar to those of the free aluminum ions [39], suggesting that the Al^{3+} ions coordinated by the sulfonic groups of the resin somehow keep their octahedral array of coordinated water molecules.

6. Aluminum in plants

The uptake of aluminum by plants has been investigated by multinuclear NMR [40,41]. The Al^{3+} ion exists in a variety of complexed forms *in vivo* and the non-destructive ^{27}Al NMR spectroscopy can be extremely helpful in their identification. Nagata *et al* [42,43] applied ^{27}Al and ^{19}F NMR to the analysis of intact tissues of tea plant (*Camellia sinensis*). This plant is an aluminum accumulator and can protect itself against aluminum injury by trapping large amounts of this element in the old leaves. They found that the dominant aluminum species in the tea leaves are catechin complexes. In order to identify the aluminum species present after absorption from soil they performed a ^{27}Al NMR study using different parts of the tea plant. This study showed the existence of two different aluminum species which were attributed to catechin and fluoride complexes. The absence of the Al-F complexes in the leaves is thought to be the result of their migration within the plant and their rapid conversion into another form in the leaves.

In a study with the leaves of hydrangea it was found that the ^{27}Al resonance peak appears at 11-12 ppm in both the intact leaves and in the extracted cell sap. The structure of the ligand chelated with Al^{3+} was identified to be citric acid in a molar ratio of 1:1 [44].

^{27}Al NMR was also applied to the detection of aluminum in lower organisms like the mycorrhizal fungus *Laccaria bicolour* [45].

7. Conclusion

The NMR spectroscopy of the Group 13 elements is a powerful non invasive technique for the study of the structure and dynamics of compounds and biological systems that interact with these metal ions. The metal ions can be native to the systems (e.g. aluminum in plants) or just be used as structural probes (e.g. thallium in proteins). Due to their quadrupolar nature, Al^{3+}, Ga^{3+} and In^{3+} are very sensitive to the symmetry of their surroundings, constituting thus a convenient report of environment of coordination. The compounds these metal ions interact with, range from low-molecular-weight molecules to macromolecules, like proteins, extending to biological tissues. *In vivo* NMR spectroscopic measurements (^{27}Al and $^{69/71}$Ga in particular) are feasible.

^{27}Al has been the most employed Group 13 nuclide in NMR studies due to its favourable magnetic resonance properties (100% abundance and fairly good receptivity). The magnetic resonance characteristics of this nuclide make it also suitable for medical applications (^{27}Al-based magnetic resonance imaging is feasible).

Abbreviations

DTPA	diethylenetriaminepentaacetic acid
DTPA-$(BuA)_2$	DTPA-N,N''-bis(butylamide)
GE	gastric emptying
H_3ppma	tris(4-(phenylphosphinato)-3-methyl-3-azabutyl)amine
L1	1,4,7-triazacyclononane-1,4,7-triyltrimethylenetris(phenylphosphinic acid)
L2	1,4,7-triazacyclodecane-1,4,7-triacetic acid
L4	1,5,9-triazacyclododecane-1,5,9-triacetic acid
L5	1,4,7-triazacyclononane-1,4,7-triyltrimethylenetris(methylphosphinic acid)
L7	1,4,7-triazacyclononane-1,4,7-triyltrimethylenetris(benzylphosphinic acid)
MRI	magnetic resonance imaging
MW	molecular weight
NMR	nuclear magnetic resonance
NODASA	1,4,7-triazacyclononane-1-succinic acid-4,7-diacetic acid
NOTA	1,4,7-triazacyclononane-1,4,7-triacetic acid
NOTMA	(*R*)-1,4,7-tris(2´-methylcarboxymethyl)-triazacyclononane
NOTP	1,4,7-triazacyclononane-1,4,7-tris(methylenephosphonic acid)
oTf	ovotransferrin
PET	positron emission tomography
sTf	serum transferrin
TACS	*cis,cis*-1,3,5-tris((2-hydroxy-5-sulfobenzyl)amino)cyclohexane
TAMS	1,1,1-tris(((2-hydroxy-5-sulfobenzyl)amino)methyl)ethane
TAPS	1,2,3-tris((2-hydroxy-5-sulfobenzyl)amino)propane
Tf	transferrin

TTHA	triethylenetetramine-N,N,N’,N’’,N’’’,N’’’-hexaacetic acid
TTHA-$(BuA)_2$	TTHA-N,N’’’-bis(butylamide)
yPk	yeast pyruvate kinase
[9]aneN_3	triazacyclononane

References

1. J. S. Cohen, J. W. Jaroszewski, O. Kaplan, J. R.-Cabello, S. W. Collier, Prog. Nucl. Mag. Res. Spec. 28 (1995) 53-85.

2. Z. Serber, V. Dötsch, Biochemistry 40 (2001) 14317-14323.

3. M. Rudin, N. Beckmann, R. Porszasz, T. Reese, D. Bochelen, A. Sauter, NMR Biomed. 12 (1999) 69-97.

4. T. Diercks, M. Coles, H. Kessler, Curr. Opin. Chem. Biol. 5 (2001) 285-291.

5. I. C. P. Smith, L. C. Stewart, Prog. Nucl. Mag. Res. Spec. 40 (2002) 1-34.

6. J. J. R. F. da Silva, R. J. P. Williams, The Biological Chemistry of the Elements, Clarendon Press, Oxford, 2002.

7. D. R. McLachlan, W. J. Lukiw, T. P. A. Kruk, in: G. Berthon (Ed.), Handbook of Metal-Ligand Interactions-Bioinorganic Medicine, Vol. 2, 1995, p.935.

8. R. J. P. Williams, Coord. Chem. Rev. 228 (2002) 93-96.

9. C. Orvig, in: G. H. Robinson (Ed.), Coordination Chemistry of Aluminum, VCH Publishers, New York, 1993, pp. 85-121.

10. R. L. Hayes, in: H.G. Seiler, H. Sigel and A. Sigel (Eds.), Handbook of Toxicity of Inorganic Compounds, Marcel Dekker, New York, 1988, p. 297.

11. J. Burgess, Chem. Soc. Rev. (1996) 85-92.

12. J.W. Akitt, in: J. Mason (Ed.), Multinuclear NMR, Plenum Press, New York, 1987, pp. 259-292.

13. J. J. Delpuech, M. R. Khadar, A. A. Peguy, P. R. Rubini, J. Am. Chem. Soc. 97 (1975) 3373-3379.

14. J. J. Delpuech, NMR of Newly Accessible Nuclei, Vol. 2, Academic Press, London, 1983.

15. J. F. Hinton, R. W. Briggs, in: R. K. Harris and B. E. Mann (Eds.), NMR and the Periodic Table, Academic Press, New York, 1978.

16. W. R. Harris, L. Messori, Coord. Chem. Rev. 228 (2002) 237-262.

17. I. Bertini, C. Luchinat, L. Messori, J. Am. Chem. Soc. 105 (1983) 1347-1350.

18. I. Bertini, L. Messori; G. C. Pellacani, M. Sola, Inorg. Chem. 27 (1988) 761-762.

19. J. M. Aramini, P. H. Krygsman, H. J. Vogel, Biochemistry 33 (1994) 3304-3311.

20. J. M. Aramini, H. J. Vogel, J. Am. Chem. Soc. 115 (1993) 245-252.

21. J. M. Aramini, H. J. Vogel, J. Am. Chem. Soc. 116 (1994) 6971-6972.

22. J. M. Aramini, D. D. McIntyre, H. J. Vogel, J. Am. Chem. Soc. 116 (1994) 11506-11511.

23. J. M. Aramini, H. J. Vogel, J. Am. Chem. Soc. 116 (1994)1988-1993.

24. J. P. Loria, T. Nowak, Biochemistry 37 (1998) 6967-6974.

25. I. Dellavia, J. Blixt, C. Dupressoir, C. Detellier, Inorg. Chem. 33 (1994) 2823-2829.

26. C. J. Broan, J. P. L. Cox, A. S. Craig, R. Kataky, D. Parker, A. Harrison, A. M. Randall, G. Ferguson, J. Chem., Soc., Perkin Trans. 2 (1991) 87-99.

27. A. S. Craig, D. Parker, H. Adams, N. A. Bailey, Chem. Comm. (1989) 1793-1794.

28. J. P. André, H. R. Maecke, M. Zehnder, L. Macko, K. G. Akyel, Chem. Commun. (1998) 1301-1302.

29. J. P. André, H. Mäcke, A. Kaspar, B. Künnecke, M. Zehnder, L. Macko, J. Inorg. Biochem. 88 (2002) 1-6.

30. E. Cole, R. C. B. Copley, J. A. K. Howard, D. Parker, G. Ferguson, J. F. Gallagher, B. Kaitner, A. Harrison, L. Royle, J. Chem., Soc., Dalton Trans. (1994) 1619-1629.

31. M. I. M. Prata, A. C. Santos, C. F. G. C. Geraldes, J. J. P. de Lima, J. Inorg. Biochem. 79 (2000) 359-363.

32. B. Achour, J. Costa, R. Delgado, E. Garrigues, C. F. G. C. Geraldes, N. Korber, F. Nepveu, M. Isabel Prata, Inorg. Chem. 37 (1998) 2729-2740.

33. P. Caravan, C. Orvig, Inorg. Chem. 36 (1997) 236-248.

34. M. P. Lowe, S. J. Rettig, C. Orvig, J. Am. Chem. Soc. 118 (1996) 10446-10456.

35. P. Yu, B. L. Phillips, M. M. Olmstead, W. H. Casey, J. Chem. Soc., Dalton Trans. (2002) 2119-2125.

36. A. Kaspar, D. Bilecen, K. Scheffler, J. Seelig, Mag. Res. Med. 36 (1996) 177-182.

37. Z. Kokot, Pharmazie, 44 (1989) 828-830.

38. R. Schwartz, A. Kaspar, J. Seelig, B. Künneke, Magn. Res. Med. 48 (2002) 255-261.

39. A. Kaspar, ^{27}Al in vivo NMR Spektroskopie und Bildgebung, PhD Thesis, University of Basel, Basel, Switzerland, 1996.

40. P. E. Pfeffer, S. I. Tu, W. V. Gerasimowicz, J. R. Cavanaugh, Plant Physiol. 80 (1986) 77-84.

41. P. E. Pfeffer, S. I. Tu, W. V. Gerasimowicz, R. T. Boswell, Planta 172 (1987) 200-208.

42. T. Nagata, M. Hayatsu, N. Kosuge, Phytochem. 31 (1991) 1215-1218.

43. T. Nagata, M. Hayatsu, N. Kosuge, Phytochem. 32 (1993) 771-775.

44. J. F. Ma; S. Hiradate, K. Nomoto, T. Iwashita, H. Matsumoto, Plant Physiol. 113 (1997) 1033-1039.

45. F. Martin, P. Rubini, R. Côté, I. Kottke, Planta 194 (1994) 241-246.

46. M. P. M. M. Catarro, Estudo de Ligandos Poliazamacrocíclicos e de seus Complexos Metálicos, PhD Thesis, University of Coimbra, Coimbra, Portugal, 1995.

47. R. C. Mathews, D. Parker, G. Ferguson, B. Kaitner, A. Harrison, L. Royle, Polyhedron 10 (1991) 1951-1953.

48. R. K. Iyer, S. B. Karweer, V. K. Jain, Magn. Reson. Chem. 27 (1989) 328-334.

Table 1 – NMR Properties of 13 Group Elements (adapted from [14])

	^{27}Al	^{69}Ga	^{71}Ga	^{113}In	^{115}In	^{203}Tl	^{205}Tl
Spin	5/2	3/2	3/2	9/2	9/2	1/2	1/2
Isotopic abundance	100	60.4	39.6	4.28	95.72	29.52	70.48
NMR freq. [a]	26.06	24.00	30.50	21.86	21.91	57.1	57.6
Quadrupole moment Q (10^{-28} m^2)	0.149	0.178	0.112	1.14	0.83	-	-
Relative receptivity R_x [b,c]	0.206, 1170	0.042, 237	0.056, 319	0.015, 84	0.332, 1890		0.1355, 769
Relative line width W_x [d]	1.00	5.94	2.35	13.55	7.18		
Relative peak height H_x [e]	100.0	3.4	11.6	0.54	22.4		

[a] In MHz for an induction of 2.348 T (^{1}H at 100 MHz)

[b] With respect to ^{1}H or ^{13}C (first and second values respectively)

[c] Computed as the ratio R of the receptivities $\alpha_x\gamma_x I_x$ (I_x+1) at constant field of the mentioned isotope and of the reference nucleus.

[d] Computed as the ratio W_x of the values taken by the function $(2I+3)Q^2/I^2(2I-1)$ for the mentioned isotope and for ^{27}Al nuclei.

[e] Computed as 100 times the ratio of the values taken by the function R_x/W_x for the mentioned isotope and for ^{27}Al nuclei.

Table 2 – NMR chemical shifts and line widths of some complexes of the Group 13 metal ions.

	^{27}Al		^{71}Ga		^{115}In	
Ligand	**δ (ppm)**	**$W_{1/2}$ (Hz)**	**δ (ppm)**	**$W_{1/2}$ (Hz)**	**δ (ppm)**	**$W_{1/2}$ (Hz)**
H_2O	0	3-20	0	53	0	375-18000
NOTA	+49 [a]	60	+171 [b]	210 [b]		
				320 (^{69}Ga)		
NODASA [c]	+47	80	+165 (^{69}Ga)	1000		
NOTP [d]			+110	434		
NOTMA [e]			+149			
L1 [b]			+132	560		
L5 [b]			+139	200		
L7 [b]			+130	1220		
L2 [f]				2000		
L4 [f]				3500		
DTPA [g]	+37.2 (1:1)	1835±20				
DTPA-(BuA)$_2$ [h]	+40.3 (1:1)	2600±20				
TTHA [i]	+35.7 (1:1)	1450±20				
	+35.7 (2:1)	1560±20				
TTHA-(BuA)$_2$ [h]	+37.8 (1:1)	3120±20	+134±5	35000±40		Very broad signal
	+37.3 (2:1)	2700±20				
H_3ppma [i]	-6.9 (1:1)	37 (1:1)				
	-13.1 (1:2)	23 (1:2)	-62.3	50	-14.7	1630
TAMS [j]			+34	3400		26000
TACS [j]			+18	1000		
TAPS [j]			+57	1230		22000

[a] [46]; [b] [30]; [c] [29],[d] [31]; [e] [47]; [f] [26]; [g] [48]; [h] [32]; [i] [34]; [j] [33]

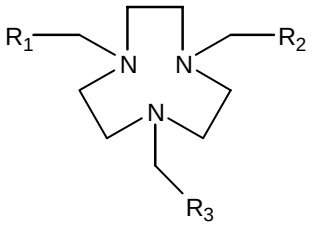

NOTA: $R_1=R_2=R_3=CH_2COOH$

NODASA: $R_1=R_2=CH_2COOH$; $R_3=CH(CH_2COOH)COOH$

NOTP: $R_1=R_2=R_3=CH_2PO_4H_2$

NOTMA: $R_1=R_2=R_3=CH(CH_3)COOH$

L1: $R_1=R_2=R_3=CH_2P(Ph)OOH$

L5: $R_1=R_2=R_3=CH_2P(Me)OOH$

L7: $R_1=R_2=R_3=CH_2P(CH_2Ph)OOH$

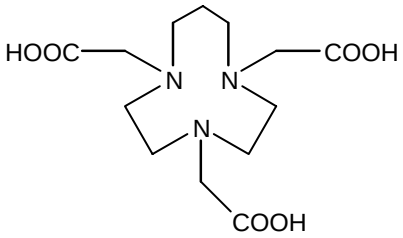

L2

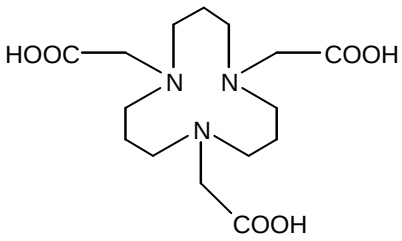

L4

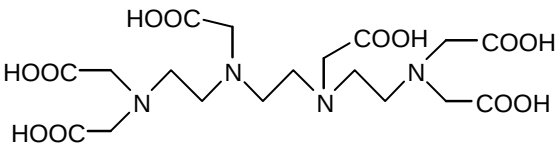

TTHA

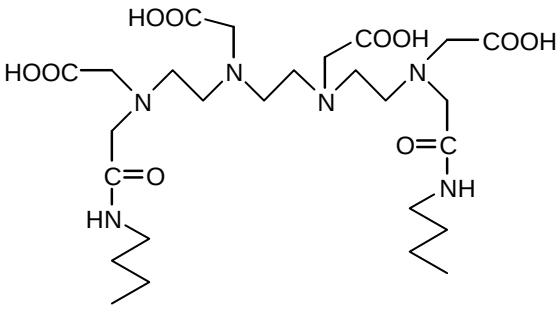

TTHA-$(BuA)_2$

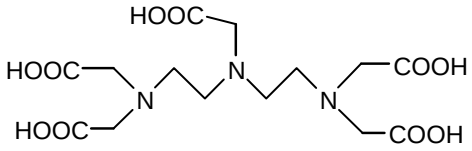

DTPA

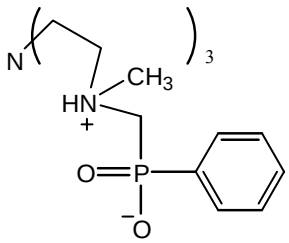

H_3ppma

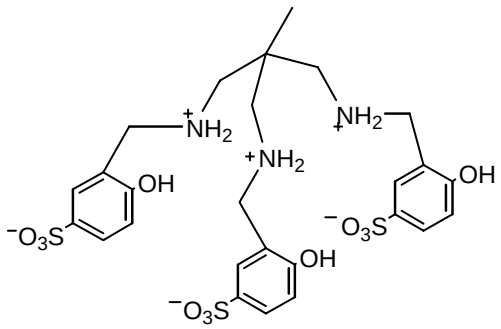

TAMS

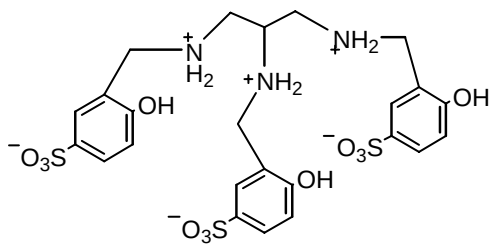

TAPS

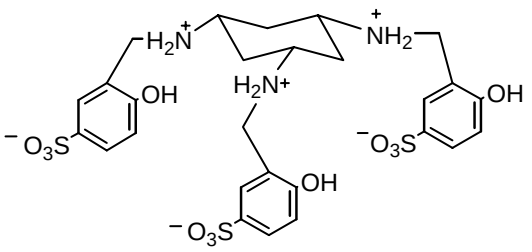

TACS

Chart 1